

Dark Matter-Induced Low-Mass Gap Black Hole Echoing LVK Observations

Shuailiang Ge^{1,2†}, Yuxin Liu^{3,4†}, Jing Shu^{1,2,5*}, Yue Zhao^{6*}

¹School of Physics and State Key Laboratory of Nuclear Physics and
Technology, Peking University, Beijing 100871, China.

²Center for High Energy Physics, Peking University, Beijing 100871,
China.

³International Centre for Theoretical Physics Asia-Pacific,
Beijing/Hangzhou, China.

⁴University of Chinese Academy of Sciences, Beijing 100190, China.

⁵Beijing Laser Acceleration Innovation Center, Huairou, Beijing, 101400,
China.

⁶Department of Physics and Astronomy, University of Utah, Salt Lake
City, Utah 84112, USA.

*Corresponding author(s). E-mail(s): jshu@pku.edu.cn;
zhaoyue@physics.utah.edu;

†The two authors have contributed equally.

Abstract

The recent detection of gravitational waves from a binary merger involving a potential low-mass gap black hole (LMBH) by LIGO-Virgo-KAGRA (LVK) Collaboration motivates investigations into mechanisms beyond conventional stellar evolution theories to account for their existence. We study a mechanism in which dark matter (DM), through its capture and accumulation inside main sequence stars, induces the formation of black holes within the mass range of $[3, 5]M_{\odot}$. We examine the distribution of these LMBHs as a function of galaxy halo mass, particularly when paired with neutron stars. This gives a distinct signature that can be tested with future gravitational wave observations. We find that a viable portion of the DM parameter space predicts a merger rate of such binaries consistent with LVK observations.

Introduction

The evolution of a main sequence (MS) star is complicated and varies depending on its mass. Stars within the mass range of $[0.5, 8]M_{\odot}$, including the Sun, typically evolve into red giants after depleting their hydrogen fuel and subsequently transform into white dwarfs (WD). MS stars with masses within $[8, 20]M_{\odot}$ possess sufficient energy to trigger supernova explosions, resulting in the violent loss of mass. This process leads to the formation of a neutron star (NS). According to the Equation of State, the maximum mass of a NS cannot exceed $3M_{\odot}$ [1–3]. When the mass of the progenitor star exceeds approximately $\sim 20M_{\odot}$ [4], the supernova explosion can be suppressed, leaving enough matter behind for the formation of an astrophysical black hole (ABH). The mass of the ABH directly produced through this process is unlikely to be smaller than $5M_{\odot}$ [4–9].¹ As a consequence, there is a gap in the mass distribution of compact objects between $[3, 5]M_{\odot}$, a feature consistent with observations of Galactic X-ray binaries [13–16].

Using traditional observation methods, searching for a low-mass gap black hole (LMBH), with mass $[3, 5]M_{\odot}$ can be challenging due to its small size and very low luminosity in electromagnetic radiation. However, gravitational wave (GW) radiation offers a new avenue for detection, even for objects located very far away from our Milky Way galaxy. Recently, the LIGO-Virgo-KAGRA (LVK) Collaboration announced the detection of a merger (GW230529) between a NS and an LMBH with a mass of $3.6_{-1.2}^{+0.8}M_{\odot}$ [17]. This breakthrough opens up a new window for investigating the existence and properties of LMBHs. Particularly, the presence of a LMBH within the mass range of $[3, 5]M_{\odot}$ may suggest phenomena beyond our current understanding, potentially necessitating novel mechanisms for their generation. For instance, such LMBHs may originate from former triple or quadruple systems [18–23], or through dynamical capture in star clusters [24–29]. Additionally, LMBHs may be identified as primordial black holes [30–34]. In this paper, we take the detection of the LMBH-NS merger as the motivation and study a novel mechanism for the LMBH production, through the dark matter (DM) capture.

The existence of DM is widely accepted, yet its properties remain in mystery. Numerous efforts are dedicated to studying the interaction between DM particles and ordinary matter, such as nucleons and electrons, especially through DM direct detection experiments [35–41]. The general interpretation of the null results in these experiments suggests a very weak interaction. On the other hand, if the interaction between DM particles and ordinary matter is too strong, the DM may not be able to freely penetrate the atmosphere and reach the experimental devices as expected. This leads to the untested extreme of DM particles with strong interactions, not explored by these experiments. In this study, we consider the DM mass m_{χ} and cross section $\sigma_{\chi\text{H}}$ between dark matter and protons in the following range,

$$m_{\chi} \in [10^4, 10^9] \text{ GeV}, \quad \sigma_{\chi\text{H}} \in [10^{-27}, 10^{-22}] \text{ cm}^2. \quad (1)$$

¹There are still debates regarding the validity of this statement, particularly concerning the fallback of outgoing matter from supernovae, as discussed in [9–12].

This overlaps with the parameter space for strongly interacting DM models which are still consistent with various experimental constraints [38, 42–44].

Although DM particles in this strongly coupled regime may evade detection in terrestrial experiments, they could readily be captured and accumulate inside an MS star. The continuous accumulation of DM particles may lead to the formation of a mini BH at the stellar center, potentially altering the ultimate fate of the star. Specifically, the presence of such a mini BH may cause a star that would otherwise become a WD or a NS to instead become a LMBH.

In this paper, we first examine the criteria for efficient DM capture and subsequent collapse to form a small BH capable of surviving Hawking radiation. We then explore how the presence of such a mini BH alters the final state of a star across various mass regimes and calculate the probability of a star being converted to a LMBH within a given halo mass. We estimate the probability distribution of detecting a LMBH-NS merger as a function of halo mass. This is a unique prediction of the DM-induced LMBH formation mechanism. With the future expansion of the GW network and enhancements in GW detector sensitivities, such a distribution serves as a discriminator to differentiate this mechanism from others. At last, we show that a substantial portion of parameter space in our DM model is capable of yielding a merger rate of LMBH-NS binaries consistent with the numbers reported by LVK.

Dark matter collapse into a black hole inside a star

As a DM particle passes through a star’s interior, it interacts with the stellar material, resulting in energy loss, which may cause it to be trapped inside by the star. A detailed study of such a capture process can be found in [45–51]. The capture probability is F_{cap} , multiplying which with the DM flux hitting the star gives the DM accumulation rate within a star [45, 49]

$$\frac{dM_{\text{acc}}}{dt} = F_{\text{cap}} \rho_{\chi} \pi R_{\text{star}}^2 \langle v_{\text{gf}} \rangle \sqrt{\frac{8}{3\pi}} \left(1 + \frac{3v_e^2}{2\langle v_{\text{gf}} \rangle^2} \right). \quad (2)$$

$\langle v_{\text{gf}} \rangle \equiv \int dv v f_{\text{gf}}(v)$ is the average velocity over the Maxwellian velocity distribution $f_{\text{gf}}(v)$ of DM in the galactic frame. $v_e = \sqrt{2GM_{\text{star}}/R_{\text{star}}}$ is the escape velocity of the star with M_{star} and R_{star} denoting the star’s mass and radius respectively and G is the gravitational constant. ρ_{χ} is the dark matter energy density near the star. For the DM parameter space Eq. (1) and the MS star mass range $[3, 5]M_{\odot}$ that we are interested in, the capture probability F_{cap} is very close to 1. More details are provided in the Supplementary Material.

If a star is located in a binary system, the DM accumulation can be enhanced by the gravitational slingshot effect from the companion star. However, this enhancement becomes significant only when the stars are in close proximity within the binary. For example, a binary of two $1.3M_{\odot}$ stars with a short orbital period of approximately 32 hours may increase the capture rate by a factor of 1.5 [52]. Consequently, we omit this effect from our study, as the DM capture process typically occurs long before the binary enters the close inspiral stage.

DM particles upon capture will continue to interact with the stellar matter, leading to further energy loss. Ultimately, they will thermalize with the stellar environment. For a $\sim 4M_\odot$ MS star, the thermalization timescale is related to the DM mass m_χ and the DM-Hydrogen scattering cross-section $\sigma_{\chi\text{H}}$ as [48]

$$t_{\text{th}} \approx 2 \times 10^{-8} \text{year} \left(\frac{m_\chi}{10^6 \text{GeV}} \right) \left(\frac{10^{-26} \text{cm}^2}{\sigma_{\chi\text{H}}} \right). \quad (3)$$

For m_χ and $\sigma_{\chi\text{H}}$ considered in the present work, the thermalization happens within a timescale much shorter than the star's lifetime. The thermalized DM particles become concentrated in the stellar core with a characteristic radius r_{th} , within which they can form thermal bound states under the star's gravitational potential $\langle V(r) \rangle = \frac{2}{3} \pi \rho_{\text{star}} G m_\chi r^2$.² The virial theorem relates this potential to the DM thermalized kinetic energy $\langle E_k \rangle = \frac{3}{2} T_{\text{star}}$ (T_{star} is the star's temperature), which implies $r_{\text{th}} \approx \sqrt{9T_{\text{star}}/(4\pi G \rho_{\text{star}} m_\chi)}$.

DM within the sphere continues to accumulate until it reaches the instability threshold, triggering a collapse. For collapsing into a BH, three criteria must collectively be satisfied: Jeans instability, self-gravitating instability, and Chandrasekhar limit [48, 49]. Detailed numerical analysis of these criteria is provided in the Supplementary Material. For the parameter space Eq. (1) and the $[3,5]M_\odot$ MS stars, it turns out that the Jeans Instability sets the most stringent threshold for the total DM mass M_{crit} within the sphere to collapse into a BH,

$$\begin{aligned} M_{\text{crit}} &= 4 \times 10^{-10} M_\odot \left(\frac{T_{\text{star}}}{10^7 \text{K}} \right)^{\frac{3}{2}} \left(\frac{m_\chi}{10^6 \text{GeV}} \right)^{-\frac{3}{2}} \left(\frac{\rho_{\text{star}}}{10^{-2} \text{kg/cm}^3} \right)^{-\frac{1}{2}} \\ &= 1.4 \times 10^{-9} M_\odot \left(\frac{M_{\text{star}}}{4M_\odot} \right)^{1.4125} \left(\frac{m_\chi}{10^6 \text{GeV}} \right)^{-\frac{3}{2}}. \end{aligned} \quad (4)$$

The second equation is obtained through scaling relations between MS stars and the Sun. Specifically, the radius and the temperature are given by $R_{\text{star}} = (M_{\text{star}}/M_\odot)^{0.8} R_\odot$ and $T_{\text{star}} = (M_{\text{star}}/M_\odot)^{0.475} T_\odot$ in accordance with the Hertzsprung-Russell diagram. The star's lifetime scales as $\tau_{\text{star}} = (M_{\text{star}}/M_\odot)^{-2.5} \tau_\odot$ [53, 54]. Additionally, we assume the star's core density follows the scaling of average density, thus the core density can be written as $\rho_{\text{star}} \propto M_{\text{star}}/R_{\text{star}}^3 \propto (M_{\text{star}}/M_\odot)^{-1.4} \rho_\odot$.

To form a BH within a star's lifetime τ_{star} , the DM accumulation rate in Eq. (2) should satisfy $dM_{\text{acc}}/dt \gtrsim M_{\text{crit}}/\tau_{\text{star}}$. This sets the criterion for the DM density in the vicinity of a star

$$\rho_{\text{crit}} \approx 4.10 \text{ GeV/cm}^3 \left(\frac{10^6 \text{GeV}}{m_\chi} \right)^{3/2} \left(\frac{M_{\text{star}}}{4M_\odot} \right)^{0.9} \left(\frac{\langle v_{\text{gf}} \rangle}{440 \text{km/s}} \right). \quad (5)$$

Here we assumed $3v_e^2/(2\langle v_{\text{gf}} \rangle^2) \gg 1$, a valid approximation for typical $\langle v_{\text{gf}} \rangle$.

²The gravitational potential of accreted DM may be neglected, as the DM energy density can only reach $\rho_\chi \sim \pi^2/12\rho_{\text{star}}$ before the gravitational collapse of DM starts.

After the mini BH forms, its mass grows by accreting both stellar material and newly captured DM particles. The former is characterized by Bondi accretion [55] and the latter depends on the DM capture rate. Additionally, the mini BH may evaporate via Hawking radiation. Incorporating these processes, the mini BH mass at the stellar core evolves as

$$\frac{dM_{\text{BH}}}{dt} = \frac{4\pi\rho_{\text{star}}(GM_{\text{BH}})^2}{c_{\text{star}}^3} + \frac{dM_{\text{acc}}}{dt} - \frac{f(M_{\text{BH}})}{(GM_{\text{BH}})^2}. \quad (6)$$

$c_{\text{star}} \approx \sqrt{T_{\text{star}}/m_{\text{H}}}$ is the speed of sound in the stellar matter. $f(M_{\text{BH}})$ is the Page factor, characterizing the strength of Hawking radiation. We take it to be $1/(74\pi)$ as the most aggressive choice, assuming the emission of all species of SM particles with gray-body corrections [48, 56]. Hawking radiation is less important compared with the first two accretion terms in Eq. (6). To see this, we take the largest DM mass in our parameter space as shown in Eq. (1), $m_{\chi} = 10^9 \text{ GeV}$, leading to the lightest mini BH (c.f. Eq. (4)) which implies the highest Hawking radiation rate and the lowest accretion rate. With this conservative choice, for a progenitor star with $4M_{\odot}$, the first two terms in Eq. (6) are $4.5 \times 10^{28} \text{ GeV/s}$ and $4.2 \times 10^{31} \text{ GeV/s}$ respectively³ while the Hawking radiation rate is only $6.2 \times 10^{10} \text{ GeV/s}$. Taking a smaller DM particle mass, the Hawking radiation is even less important. Thus, for the parameter space in Eq. (1), the mini BH always persists, potentially altering the fate of the host MS star.

Low-mass gap black hole and a possible dark matter solution

If no DM-induced BH forms in the center, a star within the mass range of $[0.5, 8]M_{\odot}$ will evolve into a red giant after depleting the hydrogen fuel, eventually transforming into a WD, based on the traditional picture. If a mini BH forms during the MS phase of a star but with a small mass, the accretion rate may not be significant enough to fully consume the star within this phase. This is due to the core maintaining a relatively constant sound speed and density throughout the MS phase. Also, radiation produced during accretion may support the in-falling matter and decrease the accretion rate from Bondi accretion, referred to be Eddington accretion [57]. However, as stated in Ref. [43], such an effect will be softened when the BH mass gets big enough where most photons are gravitationally trapped, which recovers the more efficient Bondi accretion and the BH will consume the star in a short time scale. Following their conclusion, a mini BH with mass $\gtrsim 10^{-10}M_{\odot}$ can consume an MS star heavier than $1M_{\odot}$ within $\mathcal{O}(\text{Gyr})$. To form such a mini BH ($\gtrsim 10^{-10}M_{\odot}$) inside a star with mass $3(5)M_{\odot}$, the DM mass needs to be $\lesssim 10^{6.7}(10^{6.9}) \text{ GeV}$. The consuming time will be shorter if the DM is lighter which induces a heavier mini BH in the center. On the other hand, when the star transitions into a red giant, the core's contraction could notably increase

³We note that as the accretion progresses, the BH grows larger, and the stellar matter accretion becomes dominant over the DM accretion. Additionally, the effect of Hawking radiation becomes increasingly negligible.

the accretion rate. In this study, we assume such an accretion is efficient enough for $[3, 5]M_\odot$ stars during the MS and/or the red giant phases, and the progenitor star will become a LMBH with comparable mass once DM initially induces a mini BH at the center. MS stars with masses beyond $8M_\odot$ possess the energy necessary to trigger supernova explosions, leading to the violent mass ejection and potentially generating a NS or an ABH. These massive stars have relatively short lifetimes. During the MS phase, it is unlikely for a mini BH to completely consume the whole star before supernova happens. Moreover, the supernova process is rapid and drastic, with the mini BH likely having minimal impact on the star's evolution during this phase. Hence, it is reasonable to assume that the evolution of these heavy MS stars remains largely unaffected even in the presence of a mini BH at the center.

Finally, it's worth noting that the presence of the Sun imposes a constraint on this model. Taking the local dark matter density as $\rho_\chi = 0.4\text{GeV}/\text{cm}^3$ and the local average velocity as 270km/s , we derive an upper limit on the DM mass of $m_\chi \leq 10^{6.1}\text{GeV}$, beyond which the Sun would already have been destroyed. This constraint aligns with the that reported in Refs. [48, 49].

Low-mass gap Black hole distribution

The spatial distribution of LMBHs depends on both the DM density profile and the spatial distribution of MS stars. Consequently, this leads to a unique prediction for the probability distribution of these LMBHs.

For the spatial distribution of the DM density $\rho_\chi(\vec{r}_g)$, we take the NFW profile [58], normalized to the galaxy halo mass M_h . The total stellar mass is related to M_h through a relationship derived from the Bolshoi-Planck simulation [59, 60]. Additionally, the spatial distribution of stars $\rho_s(\vec{r}_g)$ depends on the type of the galaxy, either disk or elliptical. The detailed descriptions of these quantities are provided in the Supplementary Material. With everything prepared, we can calculate the probability of a star with mass between $[3, 5]M_\odot$ within a galaxy of mass M_h becoming a LMBH during its lifetime,

$$\mathcal{P}(M_h) = \frac{N_{\text{BH}}^{\text{LM}}(M_h)}{N_{\text{star}}^{\text{LM}}(M_h)}. \quad (7)$$

The denominator is the total number of stars with mass between $[3, 5]M_\odot$,

$$N_{\text{star}}^{\text{LM}}(M_h) = \int_{3M_\odot}^{5M_\odot} \frac{dM_{\text{star}}}{\langle M_{\text{star}} \rangle} \frac{dn_{\text{star}}}{dM_{\text{star}}} \int dV \rho_s(\vec{r}_g). \quad (8)$$

Here the volume integration extends to the virial radius of the galaxy $R_{\text{vir}}(M_h)$. We take the star mass distribution $\frac{dn_{\text{star}}}{dM_{\text{star}}}$ following the initial mass function (IMF) [60, 61],

$$\frac{dn_{\text{star}}}{dM_{\text{star}}} \propto M_{\text{star}}^{-2.3}, \quad 0.5M_\odot \leq M_{\text{star}} < 100M_\odot. \quad (9)$$

The IMF is normalized by the averaged star mass $\langle M_{\text{star}} \rangle = \int dM_{\text{star}} \frac{dn_{\text{star}}}{dM_{\text{star}}} M_{\text{star}}$, whose integration range runs for all star masses. This normalization factor will eventually be canceled in our calculation. Additionally, the numerator of Eq. (7) is the

number of stars in the same mass range but will become LMBHs through DM capture,

$$N_{\text{BH}}^{\text{LM}}(M_{\text{h}}) = \int_{3M_{\odot}}^{5M_{\odot}} \frac{dM_{\text{star}}}{\langle M_{\text{star}} \rangle} \frac{dn_{\text{star}}}{dM_{\text{star}}} \times \int dV \rho_{\text{s}}(\vec{r}_{\text{g}}) \Theta[\rho_{\chi}(\vec{r}_{\text{g}}) - \rho_{\text{crit}}(\vec{r}_{\text{g}}, M_{\text{star}})]. \quad (10)$$

In Fig. 1, we take several benchmarks for DM masses and show the probability of a star with mass between $[3, 5] M_{\odot}$ to become a LMBH as a function of the halo mass. We see that almost all stars in this mass range could become LMBHs if the DM mass is large enough. This is also consistent with the DM mass upper limit imposed by the survival of the Sun.

Next, we calculate the relative probability distribution of LMBHs as a function of logarithmic halo mass,

$$\mathcal{E}(M_{\text{h}}) = \frac{\frac{dn}{d \log [M_{\text{h}}]} N_{\text{BH}}^{\text{LM}}(M_{\text{h}})}{\int d \log [M_{\text{h}}] \frac{dn}{d \log [M_{\text{h}}]} N_{\text{BH}}^{\text{LM}}(M_{\text{h}})}. \quad (11)$$

Here the halo mass distribution $\frac{dn}{d \log [M_{\text{h}}]}$ is taken as the Sheth-Tormen distribution at $z = 0$ [60, 62]. We show the result of $\mathcal{E}(M_{\text{h}})$ in Fig. 2. We emphasize that the relative probability distribution, $\mathcal{E}(M_{\text{h}})$ in Eq.(11), is a unique prediction in this mechanism, which serves as an excellent discriminator to distinguish this mechanism from other LMBH formation mechanisms.

Binary event rate estimation

One useful way to search for a LMBH in a distant galaxy is through GW radiation emitted when it merges with a compact object. The waveform during the merger offers valuable insights for identifying the properties of the binary system, especially the masses involved. In this section, we take LMBH-NS binaries as a benchmark and estimate their merger rate.

The formation and evolution of binaries involve several astrophysical uncertainties, leading to large error bars in the predictions for binary merger rates. For instance, the merger rate for an ABH-NS binary can vary widely, from 0.1 to $800 \text{Gpc}^{-3} \text{yr}^{-1}$ for isolated binaries [63–66], and from 0.1 to $100 \text{Gpc}^{-3} \text{yr}^{-1}$ for binaries in dynamical environments such as globular clusters [28, 66–69].

In order to reduce the uncertainty, we compare the merger rates of two distinct binary systems: the LMBH-NS binary and the ABH-NS binary. The masses of LMBH and ABH are related to the corresponding progenitor stars in different ways. The LMBH originates from a progenitor star with a mass between $[3, 5] M_{\odot}$ induced by DM. The LMBH and its progenitor star are approximately equal in mass, which is motivated by the expectation that no drastic explosion should occur when such a low-mass MS star evolves to its final stage⁴. While the ABH arises from a progenitor star

⁴Particularly, when the DM mass $m_{\chi} < 10^6 \text{ GeV}$, the mini BH can swallow the progenitor star within 1 Gyr [43, 57], before it turns into a red giant.

with a mass between $[20, 80]M_\odot$ which loses a significant fraction of mass through supernova explosion, resulting in an ABH heavier than $5M_\odot$ and lighter than approximately $20M_\odot$. As demonstrated in Refs. [60, 70–72], the ABH mass correlates with the original MS star mass by a factor of $O(1)$, typically centered around 4. To simplify our estimation, we take $M_{\text{ABH}} = M_{\text{star}}/4$.

To compare the LMBH-NS rate with the ABH-NS rate, several assumptions need to be made. The mass distribution of progenitor stars follows the IMF described in Eq. (9). We assume that this scaling is preserved in binary systems containing a NS before the progenitor star evolves into a BH. Moreover, during the ABH formation, the supernova explosion typically leads to a significant kick. Such effects could mildly increase the merger rate, as the kick induces a non-trivial eccentricity, accelerating the energy loss rate via gravitational waves. However, the kick may also create too much kinetic energy, causing the binary to become unbound, thereby decreasing the merger rate [63, 66, 73]. Overall, this effect may alter the merger rate of ABH-NS binaries by a factor ranging from approximately 0.1 to 1.2. For an order-of-magnitude estimation, we consider this factor to be 1. Under these assumptions, we find that the number density of LMBH-NS binaries is approximately 6.84 times greater than that of ABH-NS binaries.

At last, a BH-NS binary with a fixed initial orbit separation merges faster for a heavier BH due to a higher GW emission rate. This affects the measured merger rates for a GW detector with an $O(1)$ yr observation period. The maximum orbital period for a BH-NS binary to merge within $\Delta t^{\text{ob}} = 1$ year under the post-Newtonian approximation is [74]

$$P_{\text{max}}^{\text{ob}}(M_{\text{BH}}) \approx \left(\frac{256\pi^{8/3} \Delta t^{\text{ob}} G^{5/3} M_{\text{BH}} M_{\text{NS}}}{5(M_{\text{BH}} + M_{\text{NS}})^{1/3}} \right)^{8/3}. \quad (12)$$

In [75], the probability distribution of close binary periods $\frac{dn}{d \log P}$ follows a Gaussian distribution, centered at $\log_{10}(P/\text{day}) = 4.8$, with a dispersion of approximately 2.3. This distribution is universal across all BH masses. Taking $M_{\text{NS}} = 1.5M_\odot$, the differences in binary number densities and merger efficiencies together yield a fudge factor $A \simeq 5.79$ when we relate the observed merger rates of ABH-NS binaries and LMBH-NS binaries. More details can be found in the Supplementary Material. Consequently, after the convolution with the halo mass distribution, one can write the rate ratio of these two types of mergers as

$$\frac{\mathcal{R}^{\text{LMBH}}}{\mathcal{R}^{\text{ABH}}} = A \frac{\int d \log [M_{\text{h}}] \frac{dn}{d \log [M_{\text{h}}]} N_{\text{BH}}^{\text{LM}}(M_{\text{h}})}{\int d \log [M_{\text{h}}] \frac{dn}{d \log [M_{\text{h}}]} N_{\text{star}}^{\text{HM}}(M_{\text{h}})}. \quad (13)$$

Here $N_{\text{star}}^{\text{HM}} = \int_{20M_\odot}^{80M_\odot} \frac{dM_{\text{star}}}{\langle M_{\text{star}} \rangle} \frac{dn_{\text{star}}}{dM_{\text{star}}} \int dV \rho_s(\vec{r}_g)$, which is the total number of heavy stars given a galaxy halo mass. Taking the central value of the ABH-NS merger rate measured by LVK as $\mathcal{R}^{\text{ABH}} = 130 \text{Gpc}^{-3} \text{yr}^{-1}$ [66], we show our predicted LMBH-NS binary merger rate as a function of DM mass in Fig. 3. It is worth mentioning that a DM with mass smaller than 10^6 GeV gives a LMBH-NS merger rate consistent with

the recent LVK's reported rate [17], $55_{-47}^{+127} \text{Gpc}^{-3} \text{yr}^{-1}$, shown as the purple band in Fig. 3.

Discussions

The detection of the LMBH-NS merger by LVK indicates the existence of LMBHs. This is a surprising result and may require a detailed study on their possible formation mechanism. We find that the strongly interacting DM model offers a potential explanation for the formation of these LMBHs. A significant portion of the parameter space gives a LMBH-NS merger rate consistent with LVK's measurement.

Moreover, whether a mini BH can form within a star and eventually convert it into a LMBH depends on the properties of the DM in the star's vicinity. This leads to a unique feature in the LMBH distribution as discussed in Eq. (11). Currently, the GW network is still in its beginning stage, and the angular resolution is not good enough to identify the host galaxy of the merger on an event-by-event basis. However, with the expansion of the GW detector network and enhancements in individual detector sensitivity, we expect more LMBH-NS mergers can be measured. Both event statistics and angular resolution have the potential for significant improvements. If the host galaxy can be identified, the distribution of LMBH-NS mergers can be directly tested. Even without event-by-event identification of the host galaxy, statistical analyses can be conducted based on the distribution of potential host galaxies from surveys like the Dark Energy Spectroscopic Instrument [76, 77]. It is conceivable that such LMBH-NS distribution could be utilized to verify or refute the LMBH formation mechanism studied here.

References

- [1] Mueller, H., Serot, B.D.: Relativistic mean field theory and the high density nuclear equation of state. *Nucl. Phys. A* **606**, 508–537 (1996) [https://doi.org/10.1016/0375-9474\(96\)00187-X](https://doi.org/10.1016/0375-9474(96)00187-X) [arXiv:nuc-th/9603037](https://arxiv.org/abs/nuc-th/9603037)
- [2] Kalogera, V., Baym, G.: The maximum mass of a neutron star. *The Astrophysical Journal* **470**(1), 61 (1996)
- [3] Godzieba, D.A., Radice, D., Bernuzzi, S.: On the maximum mass of neutron stars and GW190814. *Astrophys. J.* **908**(2), 122 (2021) <https://doi.org/10.3847/1538-4357/abd4dd> [arXiv:2007.10999](https://arxiv.org/abs/2007.10999) [astro-ph.HE]
- [4] Belczynski, K., Wiktorowicz, G., Fryer, C., Holz, D., Kalogera, V.: Missing Black Holes Unveil The Supernova Explosion Mechanism. *Astrophys. J.* **757**, 91 (2012) <https://doi.org/10.1088/0004-637X/757/1/91> [arXiv:1110.1635](https://arxiv.org/abs/1110.1635) [astro-ph.GA]
- [5] O'Connor, E., Ott, C.D.: Black Hole Formation in Failing Core-Collapse Supernovae. *Astrophys. J.* **730**, 70 (2011) <https://doi.org/10.1088/0004-637X/730/2/70> [arXiv:1010.5550](https://arxiv.org/abs/1010.5550) [astro-ph.HE]
- [6] Fryer, C.L., Belczynski, K., Wiktorowicz, G., Dominik, M., Kalogera, V., Holz, D.E.: Compact Remnant Mass Function: Dependence on the Explosion Mechanism and Metallicity. *Astrophys. J.* **749**, 91 (2012) <https://doi.org/10.1088/0004-637X/749/1/91> [arXiv:1110.1726](https://arxiv.org/abs/1110.1726) [astro-ph.SR]
- [7] Janka, H.-T.: Explosion Mechanisms of Core-Collapse Supernovae. *Ann. Rev. Nucl. Part. Sci.* **62**, 407–451 (2012) <https://doi.org/10.1146/annurev-nucl-102711-094901> [arXiv:1206.2503](https://arxiv.org/abs/1206.2503) [astro-ph.SR]
- [8] Müller, B., Heger, A., Liptai, D., Cameron, J.B.: A simple approach to the supernova progenitor–explosion connection. *Mon. Not. Roy. Astron. Soc.* **460**(1), 742–764 (2016) <https://doi.org/10.1093/mnras/stw1083> [arXiv:1602.05956](https://arxiv.org/abs/1602.05956) [astro-ph.SR]
- [9] Ertl, T., Woosley, S.E., Sukhbold, T., Janka, H.-T.: The Explosion of Helium Stars Evolved With Mass Loss (2019) <https://doi.org/10.3847/1538-4357/ab6458> [arXiv:1910.01641](https://arxiv.org/abs/1910.01641) [astro-ph.HE]
- [10] Mandel, I., Müller, B.: Simple recipes for compact remnant masses and natal kicks. *Mon. Not. Roy. Astron. Soc.* **499**(3), 3214–3221 (2020) <https://doi.org/10.1093/mnras/staa3043> [arXiv:2006.08360](https://arxiv.org/abs/2006.08360) [astro-ph.HE]
- [11] Antoniadis, J., Aguilera-Dena, D.R., Vigna-Gómez, A., Kramer, M., Langer, N., Müller, B., Tauris, T.M., Wang, C., Xu, X.-T.: Explodability fluctuations of massive stellar cores enable asymmetric compact object mergers such as GW190814. *Astron. Astrophys.* **657**, 6 (2022) <https://doi.org/10.1051/0004-6361/202142322>

- [arXiv:2110.01393](https://arxiv.org/abs/2110.01393) [astro-ph.HE]
- [12] Sukhbold, T., Ertl, T., Woosley, S.E., Brown, J.M., Janka, H.-T.: Core-Collapse Supernovae from 9 to 120 Solar Masses Based on Neutrino-powered Explosions. *Astrophys. J.* **821**(1), 38 (2016) <https://doi.org/10.3847/0004-637X/821/1/38> [arXiv:1510.04643](https://arxiv.org/abs/1510.04643) [astro-ph.HE]
- [13] Bailyn, C.D., Jain, R.K., Coppi, P., Orosz, J.A.: The Mass distribution of stellar black holes. *Astrophys. J.* **499**, 367 (1998) <https://doi.org/10.1086/305614> [arXiv:astro-ph/9708032](https://arxiv.org/abs/astro-ph/9708032)
- [14] Ozel, F., Psaltis, D., Narayan, R., McClintock, J.E.: The Black Hole Mass Distribution in the Galaxy. *Astrophys. J.* **725**, 1918–1927 (2010) <https://doi.org/10.1088/0004-637X/725/2/1918> [arXiv:1006.2834](https://arxiv.org/abs/1006.2834) [astro-ph.GA]
- [15] Farr, W.M., Sravan, N., Cantrell, A., Kreidberg, L., Bailyn, C.D., Mandel, I., Kalogera, V.: The Mass Distribution of Stellar-Mass Black Holes. *Astrophys. J.* **741**, 103 (2011) <https://doi.org/10.1088/0004-637X/741/2/103> [arXiv:1011.1459](https://arxiv.org/abs/1011.1459) [astro-ph.GA]
- [16] Kreidberg, L., Bailyn, C.D., Farr, W.M., Kalogera, V.: Mass Measurements of Black Holes in X-Ray Transients: Is There a Mass Gap? *Astrophys. J.* **757**, 36 (2012) <https://doi.org/10.1088/0004-637X/757/1/36> [arXiv:1205.1805](https://arxiv.org/abs/1205.1805) [astro-ph.HE]
- [17] Abbott, R., et al.: Observation of Gravitational Waves from the Coalescence of a 2.5 – 4.5 M_{\odot} Compact Object and a Neutron Star (2024) [arXiv:2404.04248](https://arxiv.org/abs/2404.04248) [astro-ph.HE]
- [18] Fragione, G., Loeb, A., Rasio, F.A.: Merging Black Holes in the Low-mass and High-mass Gaps from 2 + 2 Quadruple Systems. *Astrophys. J. Lett.* **895**(1), 15 (2020) <https://doi.org/10.3847/2041-8213/ab9093> [arXiv:2002.11278](https://arxiv.org/abs/2002.11278) [astro-ph.GA]
- [19] Lu, W., Beniamini, P., Bonnerot, C.: On the formation of GW190814. *Mon. Not. Roy. Astron. Soc.* **500**(2), 1817–1832 (2020) <https://doi.org/10.1093/mnras/staa3372> [arXiv:2009.10082](https://arxiv.org/abs/2009.10082) [astro-ph.HE]
- [20] Liu, B., Lai, D.: Hierarchical Black-Hole Mergers in Multiple Systems: Constrain the Formation of GW190412, GW190814 and GW190521-like events. *Mon. Not. Roy. Astron. Soc.* **502**(2), 2049–2064 (2021) <https://doi.org/10.1093/mnras/stab178> [arXiv:2009.10068](https://arxiv.org/abs/2009.10068) [astro-ph.HE]
- [21] Vynatheya, P., Hamers, A.S.: How Important Is Secular Evolution for Black Hole and Neutron Star Mergers in 2+2 and 3+1 Quadruple-star Systems? *Astrophys. J.* **926**(2), 195 (2022) <https://doi.org/10.3847/1538-4357/ac4892> [arXiv:2110.14680](https://arxiv.org/abs/2110.14680) [astro-ph.HE]

- [22] Gayathri, V., Bartos, I., Rosswog, S., Miller, M.C., Veske, D., Lu, W., Marka, S.: Do gravitational wave observations in the lower mass gap favor a hierarchical triple origin? (2023) [arXiv:2307.09097](https://arxiv.org/abs/2307.09097) [astro-ph.HE]
- [23] Bartos, I., Rosswog, S., Gayathri, V., Miller, M.C., Veske, D., Marka, S.: Hierarchical Triples as Early Sources of r -process Elements (2023) [arXiv:2302.10350](https://arxiv.org/abs/2302.10350) [astro-ph.HE]
- [24] Clausen, D., Sigurdsson, S., Chernoff, D.F.: Black Hole-Neutron Star Mergers in Globular Clusters. *Mon. Not. Roy. Astron. Soc.* **428**, 3618 (2013) <https://doi.org/10.1093/mnras/sts295> [arXiv:1210.8153](https://arxiv.org/abs/1210.8153) [astro-ph.HE]
- [25] Gupta, A., Gerosa, D., Arun, K.G., Berti, E., Farr, W.M., Sathyaprakash, B.S.: Black holes in the low mass gap: Implications for gravitational wave observations. *Phys. Rev. D* **101**(10), 103036 (2020) <https://doi.org/10.1103/PhysRevD.101.103036> [arXiv:1909.05804](https://arxiv.org/abs/1909.05804) [gr-qc]
- [26] Ye, C.S., Fong, W.-f., Kremer, K., Rodriguez, C.L., Chatterjee, S., Fragione, G., Rasio, F.A.: On the Rate of Neutron Star Binary Mergers from Globular Clusters. *Astrophys. J. Lett.* **888**(1), 10 (2020) <https://doi.org/10.3847/2041-8213/ab5dc5> [arXiv:1910.10740](https://arxiv.org/abs/1910.10740) [astro-ph.HE]
- [27] Rastello, S., Mapelli, M., Di Carlo, U.N., Giacobbo, N., Santoliquido, F., Spera, M., Ballone, A., Iorio, G.: Dynamics of black hole–neutron star binaries in young star clusters. *Mon. Not. Roy. Astron. Soc.* **497**(2), 1563–1570 (2020) <https://doi.org/10.1093/mnras/staa2018> [arXiv:2003.02277](https://arxiv.org/abs/2003.02277) [astro-ph.HE]
- [28] Sedda, M.A.: Dissecting the properties of neutron star - black hole mergers originating in dense star clusters. *Commun. Phys.* **3**, 43 (2020) <https://doi.org/10.1038/s42005-020-0310-x> [arXiv:2003.02279](https://arxiv.org/abs/2003.02279) [astro-ph.GA]
- [29] Arca Sedda, M.: Dynamical Formation of the GW190814 Merger. *Astrophys. J. Lett.* **908**(2), 38 (2021) <https://doi.org/10.3847/2041-8213/abdfcd> [arXiv:2102.03364](https://arxiv.org/abs/2102.03364) [astro-ph.HE]
- [30] Bird, S., Cholis, I., Muñoz, J.B., Ali-Haïmoud, Y., Kamionkowski, M., Kovetz, E.D., Raccanelli, A., Riess, A.G.: Did LIGO detect dark matter? *Phys. Rev. Lett.* **116**(20), 201301 (2016) <https://doi.org/10.1103/PhysRevLett.116.201301> [arXiv:1603.00464](https://arxiv.org/abs/1603.00464) [astro-ph.CO]
- [31] Clesse, S., García-Bellido, J.: The clustering of massive Primordial Black Holes as Dark Matter: measuring their mass distribution with Advanced LIGO. *Phys. Dark Univ.* **15**, 142–147 (2017) <https://doi.org/10.1016/j.dark.2016.10.002> [arXiv:1603.05234](https://arxiv.org/abs/1603.05234) [astro-ph.CO]
- [32] Sasaki, M., Suyama, T., Tanaka, T., Yokoyama, S.: Primordial Black Hole Scenario for the Gravitational-Wave Event GW150914. *Phys. Rev.*

- Lett. **117**(6), 061101 (2016) <https://doi.org/10.1103/PhysRevLett.117.061101> [arXiv:1603.08338](https://arxiv.org/abs/1603.08338) [astro-ph.CO]. [Erratum: Phys.Rev.Lett. 121, 059901 (2018)]
- [33] Kashlinsky, A.: LIGO gravitational wave detection, primordial black holes and the near-IR cosmic infrared background anisotropies. *Astrophys. J. Lett.* **823**(2), 25 (2016) <https://doi.org/10.3847/2041-8205/823/2/L25> [arXiv:1605.04023](https://arxiv.org/abs/1605.04023) [astro-ph.CO]
- [34] Clesse, S., Garcia-Bellido, J.: GW190425, GW190521 and GW190814: Three candidate mergers of primordial black holes from the QCD epoch. *Phys. Dark Univ.* **38**, 101111 (2022) <https://doi.org/10.1016/j.dark.2022.101111> [arXiv:2007.06481](https://arxiv.org/abs/2007.06481) [astro-ph.CO]
- [35] Abrams, D., *et al.*: Exclusion Limits on the WIMP Nucleon Cross-Section from the Cryogenic Dark Matter Search. *Phys. Rev. D* **66**, 122003 (2002) <https://doi.org/10.1103/PhysRevD.66.122003> [arXiv:astro-ph/0203500](https://arxiv.org/abs/astro-ph/0203500)
- [36] Aprile, E., *et al.*: First Dark Matter Search Results from the XENON1T Experiment. *Phys. Rev. Lett.* **119**(18), 181301 (2017) <https://doi.org/10.1103/PhysRevLett.119.181301> [arXiv:1705.06655](https://arxiv.org/abs/1705.06655) [astro-ph.CO]
- [37] Cui, X., *et al.*: Dark Matter Results From 54-Ton-Day Exposure of PandaX-II Experiment. *Phys. Rev. Lett.* **119**(18), 181302 (2017) <https://doi.org/10.1103/PhysRevLett.119.181302> [arXiv:1708.06917](https://arxiv.org/abs/1708.06917) [astro-ph.CO]
- [38] Kavanagh, B.J.: Earth scattering of superheavy dark matter: Updated constraints from detectors old and new. *Phys. Rev. D* **97**(12), 123013 (2018) <https://doi.org/10.1103/PhysRevD.97.123013> [arXiv:1712.04901](https://arxiv.org/abs/1712.04901) [hep-ph]
- [39] Digman, M.C., Cappiello, C.V., Beacom, J.F., Hirata, C.M., Peter, A.H.G.: Not as big as a barn: Upper bounds on dark matter-nucleus cross sections. *Phys. Rev. D* **100**(6), 063013 (2019) <https://doi.org/10.1103/PhysRevD.100.063013> [arXiv:1907.10618](https://arxiv.org/abs/1907.10618) [hep-ph]. [Erratum: Phys.Rev.D 106, 089902 (2022)]
- [40] Clark, M., Depoian, A., Elshimy, B., Kopec, A., Lang, R.F., Li, S., Qin, J.: Direct Detection Limits on Heavy Dark Matter. *Phys. Rev. D* **102**(12), 123026 (2020) <https://doi.org/10.1103/PhysRevD.102.123026> [arXiv:2009.07909](https://arxiv.org/abs/2009.07909) [hep-ph]
- [41] Carney, D., *et al.*: Snowmass2021 cosmic frontier white paper: Ultraheavy particle dark matter. *SciPost Phys. Core* **6**, 075 (2023) <https://doi.org/10.21468/SciPostPhysCore.6.4.075> [arXiv:2203.06508](https://arxiv.org/abs/2203.06508) [hep-ph]
- [42] Albuquerque, I.F.M., Baudis, L.: Direct detection constraints on superheavy dark matter. *Phys. Rev. Lett.* **90**, 221301 (2003) <https://doi.org/10.1103/PhysRevLett.90.221301> [arXiv:astro-ph/0301188](https://arxiv.org/abs/astro-ph/0301188). [Erratum: Phys.Rev.Lett. 91, 229903 (2003)]

- [43] Caplan, M.E., Bellinger, E.P., Santarelli, A.D.: Is there a black hole in the center of the Sun? *Astrophys. Space Sci.* **369**(1), 8 (2024) <https://doi.org/10.1007/s10509-024-04270-1> [arXiv:2312.07647](https://arxiv.org/abs/2312.07647) [astro-ph.SR]
- [44] Bhoonah, A., Bramante, J., Courtman, B., Song, N.: Etched plastic searches for dark matter. *Phys. Rev. D* **103**(10), 103001 (2021) <https://doi.org/10.1103/PhysRevD.103.103001> [arXiv:2012.13406](https://arxiv.org/abs/2012.13406) [hep-ph]
- [45] Gould, A.: Resonant Enhancements in WIMP Capture by the Earth. *Astrophys. J.* **321**, 571 (1987) <https://doi.org/10.1086/165653>
- [46] Jungman, G., Kamionkowski, M., Griest, K.: Supersymmetric dark matter. *Phys. Rept.* **267**, 195–373 (1996) [https://doi.org/10.1016/0370-1573\(95\)00058-5](https://doi.org/10.1016/0370-1573(95)00058-5) [arXiv:hep-ph/9506380](https://arxiv.org/abs/hep-ph/9506380)
- [47] Garani, R., Palomares-Ruiz, S.: Dark matter in the Sun: scattering off electrons vs nucleons. *JCAP* **05**, 007 (2017) <https://doi.org/10.1088/1475-7516/2017/05/007> [arXiv:1702.02768](https://arxiv.org/abs/1702.02768) [hep-ph]
- [48] Acevedo, J.F., Bramante, J., Goodman, A., Kopp, J., Opferkuch, T.: Dark Matter, Destroyer of Worlds: Neutrino, Thermal, and Existential Signatures from Black Holes in the Sun and Earth. *JCAP* **04**, 026 (2021) <https://doi.org/10.1088/1475-7516/2021/04/026> [arXiv:2012.09176](https://arxiv.org/abs/2012.09176) [hep-ph]
- [49] Ray, A.: Celestial objects as strongly-interacting nonannihilating dark matter detectors. *Phys. Rev. D* **107**(8), 083012 (2023) <https://doi.org/10.1103/PhysRevD.107.083012> [arXiv:2301.03625](https://arxiv.org/abs/2301.03625) [hep-ph]
- [50] Leane, R.K., Smirnov, J.: Dark matter capture in celestial objects: treatment across kinematic and interaction regimes. *JCAP* **12**, 040 (2023) <https://doi.org/10.1088/1475-7516/2023/12/040> [arXiv:2309.00669](https://arxiv.org/abs/2309.00669) [hep-ph]
- [51] Bhattacharya, S., Miller, A.L., Ray, A.: Continuous Gravitational Waves: A New Window to Look for Heavy Non-annihilating Dark Matter (2024) [arXiv:2403.13886](https://arxiv.org/abs/2403.13886) [hep-ph]
- [52] Brayeur, L., Tinyakov, P.: Enhancement of dark matter capture by neutron stars in binary systems. *Phys. Rev. Lett.* **109**, 061301 (2012) <https://doi.org/10.1103/PhysRevLett.109.061301> [arXiv:1111.3205](https://arxiv.org/abs/1111.3205) [astro-ph.CO]
- [53] Lecchini, S.: How Dwarfs Became Giants: The Discovery of the Mass-Luminosity Relation. *Bern Studies in the History and Philosophy of Science*, ??? (2007)
- [54] Hansen, C.J., Kawaler, S.D., Trimble, V.: *Stellar interiors: physical principles, structure, and evolution*. Springer, ??? (2012)
- [55] Bondi, H., Hoyle, F.: On the mechanism of accretion by stars. *Mon. Not. Roy.*

Astron. Soc. **104**, 273 (1944)

- [56] Arbey, A., Auffinger, J.: Physics Beyond the Standard Model with Black-Hawk v2.0. *Eur. Phys. J. C* **81**, 910 (2021) <https://doi.org/10.1140/epjc/s10052-021-09702-8> arXiv:2108.02737 [gr-qc]
- [57] Bellinger, E.P., Caplan, M.E., Ryu, T., Bollimpalli, D., Ball, W.H., Kühnel, F., Farmer, R., Mink, S.E., Christensen-Dalsgaard, J.: Solar Evolution Models with a Central Black Hole. *Astrophys. J.* **959**(2), 113 (2023) <https://doi.org/10.3847/1538-4357/ad04de> arXiv:2312.06782 [astro-ph.SR]
- [58] Navarro, J.F., Frenk, C.S., White, S.D.M.: A Universal density profile from hierarchical clustering. *Astrophys. J.* **490**, 493–508 (1997) <https://doi.org/10.1086/304888> arXiv:astro-ph/9611107
- [59] Behroozi, P., Wechsler, R.H., Hearin, A.P., Conroy, C.: UniverseMachine: The correlation between galaxy growth and dark matter halo assembly from $z = 0–10$. *Mon. Not. Roy. Astron. Soc.* **488**(3), 3143–3194 (2019) <https://doi.org/10.1093/mnras/stz1182> arXiv:1806.07893
- [60] Cui, W., Huang, F., Shu, J., Zhao, Y.: Stochastic gravitational wave background from PBH-ABH mergers *. *Chin. Phys. C* **46**(5), 055103 (2022) <https://doi.org/10.1088/1674-1137/ac4cab> arXiv:2108.04279 [astro-ph.CO]
- [61] Kroupa, P.: On the variation of the initial mass function. *Mon. Not. Roy. Astron. Soc.* **322**, 231 (2001) <https://doi.org/10.1046/j.1365-8711.2001.04022.x> arXiv:astro-ph/0009005
- [62] Sheth, R.K., Tormen, G.: Large scale bias and the peak background split. *Mon. Not. Roy. Astron. Soc.* **308**, 119 (1999) <https://doi.org/10.1046/j.1365-8711.1999.02692.x> arXiv:astro-ph/9901122
- [63] Belczynski, K., Kalogera, V., Bulik, T.: A Comprehensive study of binary compact objects as gravitational wave sources: Evolutionary channels, rates, and physical properties. *Astrophys. J.* **572**, 407–431 (2001) <https://doi.org/10.1086/340304> arXiv:astro-ph/0111452
- [64] Samsing, J., Hotokezaka, K.: Populating the Black Hole Mass Gaps in Stellar Clusters: General Relations and Upper Limits. *Astrophys. J.* **923**(1), 126 (2021) <https://doi.org/10.3847/1538-4357/ac2b27> arXiv:2006.09744 [astro-ph.HE]
- [65] Broekgaarden, F.S., Berger, E., Neijssel, C.J., Vigna-Gómez, A., Chattopadhyay, D., Stevenson, S., Chruslinska, M., Justham, S., Mink, S.E., Mandel, I.: Impact of massive binary star and cosmic evolution on gravitational wave observations I: black hole–neutron star mergers. *Mon. Not. Roy. Astron. Soc.* **508**(4), 5028–5063 (2021) <https://doi.org/10.1093/mnras/stab2716> arXiv:2103.02608 [astro-ph.HE]

- [66] Abbott, R., *et al.*: Observation of Gravitational Waves from Two Neutron Star–Black Hole Coalescences. *Astrophys. J. Lett.* **915**(1), 5 (2021) <https://doi.org/10.3847/2041-8213/ac082e> arXiv:2106.15163 [astro-ph.HE]
- [67] Portegies Zwart, S.F., McMillan, S.: Black hole mergers in the universe. *Astrophys. J. Lett.* **528**, 17 (2000) <https://doi.org/10.1086/312422> arXiv:astro-ph/9910061
- [68] Antonini, F., Murray, N., Mikkola, S.: Black hole triple dynamics: breakdown of the orbit average approximation and implications for gravitational wave detections. *Astrophys. J.* **781**, 45 (2014) <https://doi.org/10.1088/0004-637X/781/1/45> arXiv:1308.3674 [astro-ph.HE]
- [69] Hoang, B.-M., Naoz, S., Kremer, K.: Neutron Star–Black Hole Mergers from Gravitational-wave Captures. *Astrophys. J.* **903**(1), 8 (2020) <https://doi.org/10.3847/1538-4357/abb66a> arXiv:2007.08531 [astro-ph.HE]
- [70] Vink, J.S., Koter, A., Lamers, H.J.G.L.M.: Mass-loss predictions for o and b stars as a function of metallicity. *Astron. Astrophys.* **369**, 574–588 (2001) <https://doi.org/10.1051/0004-6361:20010127> arXiv:astro-ph/0101509
- [71] Vink, J.S., Muijres, L.E., Anthonisse, B., Koter, A., Graefener, G., Langer, N.: Wind modelling of very massive stars up to 300 solar masses. *Astron. Astrophys.* **531**, 132 (2011) <https://doi.org/10.1051/0004-6361/201116614> arXiv:1105.0556 [astro-ph.SR]
- [72] Chen, Y., Bressan, A., Girardi, L., Marigo, P., Kong, X., Lanza, A.: parsec evolutionary tracks of massive stars up to $350M_{\odot}$ at metallicities $0.0001 \leq Z \leq 0.04$. *Monthly Notices of the Royal Astronomical Society* **452**(1), 1068–1080 (2015) <https://doi.org/10.1093/mnras/stv1281> <https://academic.oup.com/mnras/article-pdf/452/1/1068/4920265/stv1281.pdf>
- [73] Tang, P.N., Eldridge, J.J., Stanway, E.R., Bray, J.C.: Dependence of Gravitational Wave Transient Rates on Cosmic Star Formation and Metallicity Evolution History. *Mon. Not. Roy. Astron. Soc.* **493**(1), 6–10 (2020) <https://doi.org/10.1093/mnras/slz183> arXiv:1912.04474 [astro-ph.GA]
- [74] Maggiore, M.: *Gravitational Waves. Vol. 1: Theory and Experiments.* Oxford University Press, ??? (2007). <https://doi.org/10.1093/acprof:oso/9780198570745.001.0001>
- [75] Tokovinin, A., Moe, M.: Formation of close binaries by disc fragmentation and migration, and its statistical modelling. *Monthly Notices of the Royal Astronomical Society* **491**(4), 5158–5171 (2020)
- [76] Abareshi, B., *et al.*: Overview of the Instrumentation for the Dark Energy Spectroscopic Instrument. *Astron. J.* **164**(5), 207 (2022) <https://doi.org/10.3847/>

- 1538-3881/ac882b arXiv:2205.10939 [astro-ph.IM]
- [77] Adame, A.G., *et al.*: Validation of the Scientific Program for the Dark Energy Spectroscopic Instrument. *Astron. J.* **167**(2), 62 (2024) <https://doi.org/10.3847/1538-3881/ad0b08> arXiv:2306.06307 [astro-ph.CO]
- [78] Bramante, J., Broerman, B., Lang, R.F., Raj, N.: Saturated Overburden Scattering and the Multiscatter Frontier: Discovering Dark Matter at the Planck Mass and Beyond. *Phys. Rev. D* **98**(8), 083516 (2018) <https://doi.org/10.1103/PhysRevD.98.083516> arXiv:1803.08044 [hep-ph]
- [79] Bramante, J., Buchanan, A., Goodman, A., Lodhi, E.: Terrestrial and Martian Heat Flow Limits on Dark Matter. *Phys. Rev. D* **101**(4), 043001 (2020) <https://doi.org/10.1103/PhysRevD.101.043001> arXiv:1909.11683 [hep-ph]
- [80] Sheth, R.K., Tormen, G.: An Excursion Set Model of Hierarchical Clustering : Ellipsoidal Collapse and the Moving Barrier. *Mon. Not. Roy. Astron. Soc.* **329**, 61 (2002) <https://doi.org/10.1046/j.1365-8711.2002.04950.x> arXiv:astro-ph/0105113
- [81] Klypin, A., Trujillo-Gomez, S., Primack, J.: Halos and galaxies in the standard cosmological model: results from the Bolshoi simulation. *Astrophys. J.* **740**, 102 (2011) <https://doi.org/10.1088/0004-637X/740/2/102> arXiv:1002.3660 [astro-ph.CO]
- [82] Prada, F., Klypin, A.A., Cuesta, A.J., Betancort-Rijo, J.E., Primack, J.: Halo concentrations in the standard LCDM cosmology. *Mon. Not. Roy. Astron. Soc.* **423**, 3018–3030 (2012) <https://doi.org/10.1111/j.1365-2966.2012.21007.x> arXiv:1104.5130 [astro-ph.CO]
- [83] White, M.J.: The Mass of a halo. *Astron. Astrophys.* **367**, 27 (2001) <https://doi.org/10.1051/0004-6361:20000357> arXiv:astro-ph/0011495
- [84] McMillan, P.J.: The mass distribution and gravitational potential of the Milky Way. *Mon. Not. Roy. Astron. Soc.* **465**(1), 76–94 (2016) <https://doi.org/10.1093/mnras/stw2759> arXiv:1608.00971 [astro-ph.GA]
- [85] Hernquist, L.: An Analytical Model for Spherical Galaxies and Bulges. *Astrophys. J.* **356**, 359 (1990) <https://doi.org/10.1086/168845>
- [86] Mo, H., van den Bosch, F.C., White, S.: *Galaxy Formation and Evolution*, (2010)
- [87] Kravtsov, A.V.: The size - virial radius relation of galaxies. *Astrophys. J. Lett.* **764**, 31 (2013) <https://doi.org/10.1088/2041-8205/764/2/L31> arXiv:1212.2980 [astro-ph.CO]

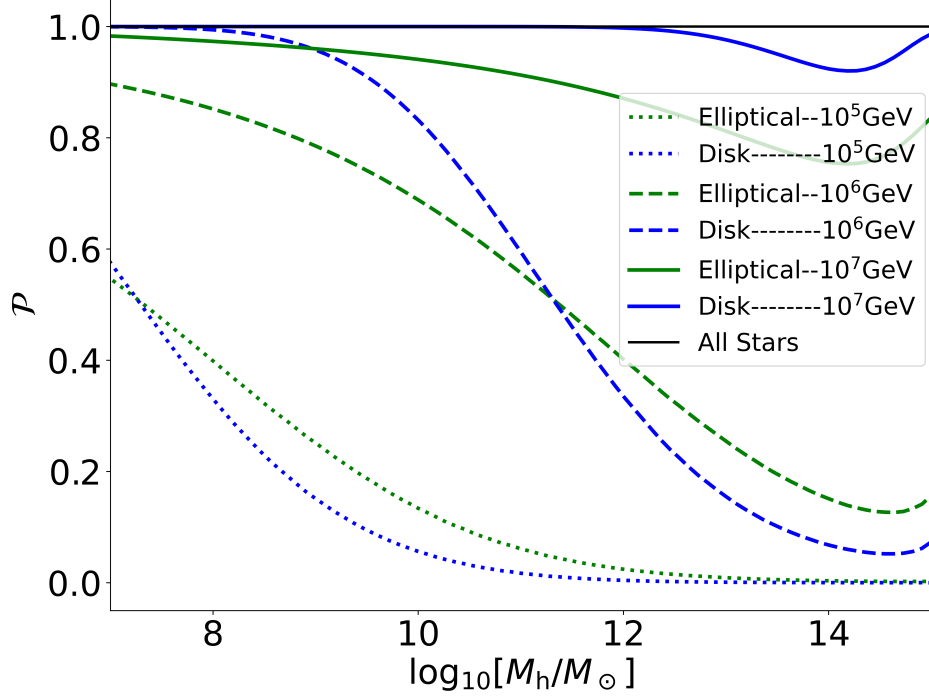


Fig. 1 With various choices of DM masses and galaxy types, we show the probability for progenitor stars within mass range $[3, 5]M_{\odot}$ to become LMBHs, as a function of the halo mass. The black line labeled as “All Star” denotes the scenario where all MS stars within the same mass range are converted into LMBHs ($\mathcal{P} = 1$).

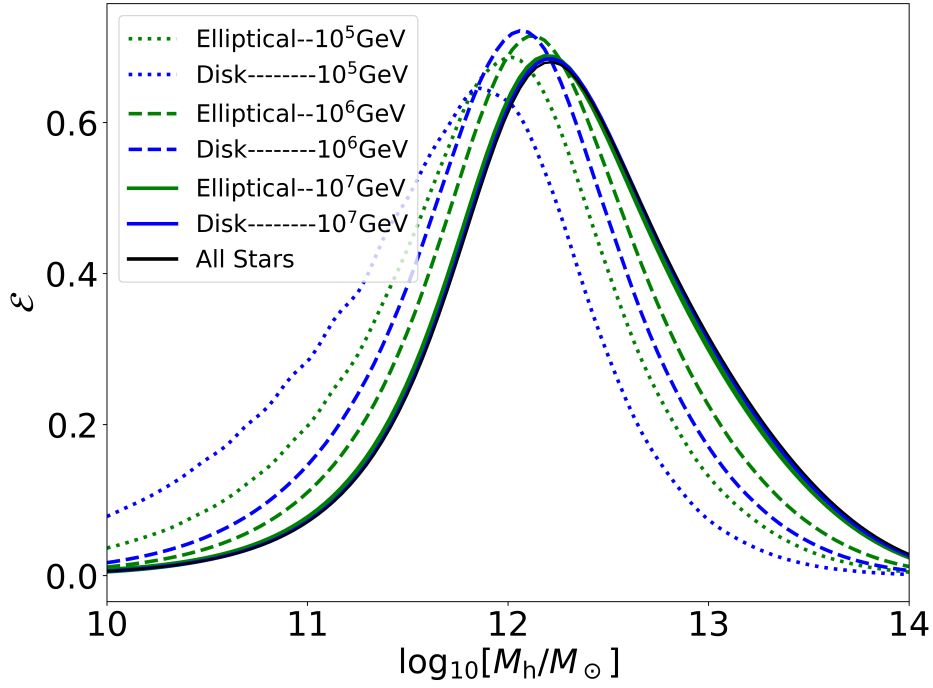


Fig. 2 With various choices of DM masses and the galaxy types, we show the relative probability distribution for $[3, 5]M_{\odot}$ LMBHs as a function of the logarithmic halo mass. The black line labeled as “All Star” denotes the scenario where all MS stars within the same mass range are converted into LMBHs.

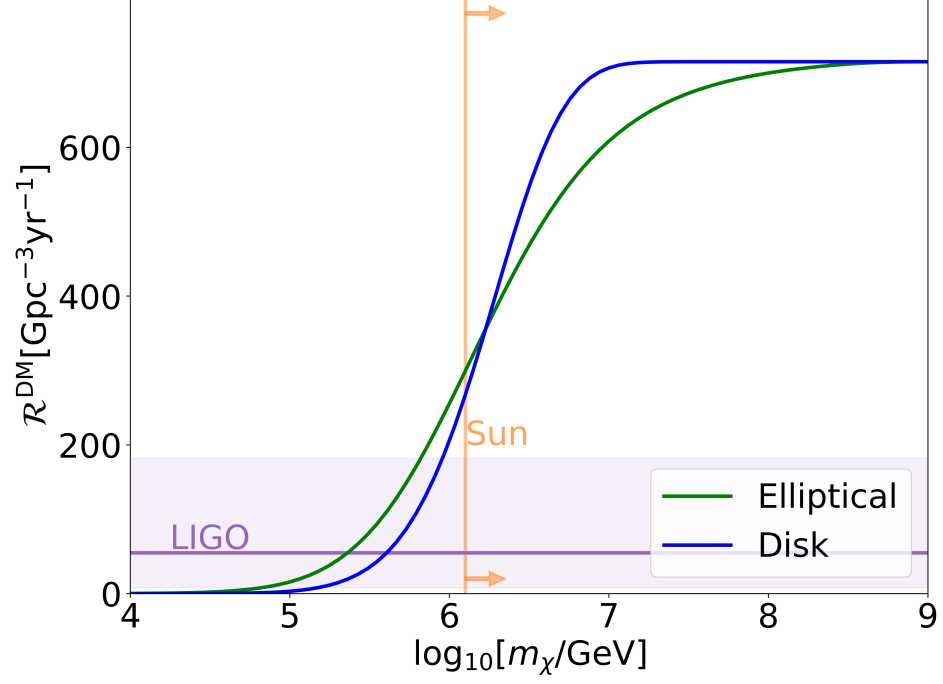


Fig. 3 For different galaxy types, we show the predicted LMBH-NS merger rate as a function of DM mass. In comparison, the purple line (band) corresponds to the merge rate (uncertainty) by LVK's recent observations [17]. The region to the right of the orange vertical line is excluded, which is the survival constraint of the Sun.

Methods

This Methods section details the mechanisms of dark matter capture within stellar bodies. It also provides explicit formulas for the criteria of gravitational collapse, as mentioned in the main text, elucidating the conditions under which such collapses are expected to occur. Additionally, the material offers insights into the galaxy number density distribution with respect to halo mass, as well as the distribution of stellar and dark matter within each galaxy. Finally, the modifications to the relative binary formation rate between two kinds of binaries (1. binaries of low-mass gap black hole and neutron star, and 2. binaries of astrophysical black hole and neutron star) are meticulously calculated.

Dark matter capture rate in the star body

In this section, we follow the calculations presented in [45, 46, 48, 49]. We simplify the interactions between DM and stellar matter as one-dimensional head-on collisions. This simplification provides a reasonable estimation of the orders of magnitude, as demonstrated in [48, 78, 79]. We first estimate the typical energy loss for each collision between a DM particle, denoted as χ , and hydrogen, the predominant component within an MS star. Assuming the initial velocity of the dark matter particle as v_i , the final velocity of the DM after a single scattering event with a hydrogen can be expressed as $v_f = v_i \sqrt{1 - z\beta}$, where β is defined as $\beta \equiv 4m_{\text{H}}m_{\chi}/(m_{\text{H}} + m_{\chi})^2$ and z is a geometric factor averaged to $z = 1/2$ for isotropic spin-independent collision angles. For the parameter space that we are interested in (refer to Eq. (1)), DM mass is always much larger than the mass of hydrogen, which leads to $\beta \approx 4 \text{ GeV}/m_{\chi}$. When DM particles pass through the star's interior, the average number of collisions can be estimated as

$$N(\theta) = \int_0^L n_{\text{H}}(r) \sigma_{\chi\text{H}} dL. \quad (14)$$

Here, θ represents the angle between the velocity of the DM particle and the radial direction \hat{r} of the star upon entry. Neglecting any change in the DM propagation direction, the distance traveled by the DM particle within the star can be expressed as $L = 2R_{\text{star}}|\cos\theta|$, where R_{star} denotes the radius of the star. Additionally, $n_{\text{H}}(r)$ denotes the hydrogen number density at a distance r from the center of the star, while $\sigma_{\chi\text{H}}$ represents the cross-section for DM-hydrogen interaction. Therefore, with a fixed angle θ , the maximum initial velocity for a DM particle to be captured is

$$v_{\text{max}}(\theta) = \frac{v_e}{(1 - z\beta_{\text{H}})^{N(\theta)/2}}. \quad (15)$$

Here v_e is the escape velocity of the star, $v_e = \sqrt{2GM_{\text{star}}/R_{\text{star}}}$, with M_{star} and R_{star} represent the mass and radius of the star, respectively.

For the DM velocity distribution, we adopt a Maxwellian distribution in the galactic frame, given by

$$f_{\text{gf}}(v) = \frac{4}{\sqrt{\pi}} \frac{v^2}{v_0^3} \exp\left(-\frac{v^2}{v_0^2}\right), \quad (16)$$

where v_0 is taken to be the circular velocity v_{cir} in the halo, which should also be the virial velocity v_{vir} according to Virial Theorem. When considering a star moving at velocity \vec{v}_{star} relative to the galactic center, the DM velocity in the star's frame requires adjustment through a Galilean transformation. Moreover, as DM particles approach the surface of the star, they experience acceleration due to the gravitational potential. For a DM particle with velocity \vec{u} at infinity in the star's frame, its velocity upon entering the stellar region becomes $v^2 = |\vec{u}|^2 + v_e^2$.

We consider a star velocity $|\vec{v}_{\text{star}}| = v_0$ within the galactic frame. Consequently, the velocity distribution of DM particles at infinitely far in the star frame, $f(u)$, can be derived through a Galilean transformation of Eq. (16), which gives

$$f(u, \phi) = \frac{1}{N^*} \frac{uv_{\text{gf}}^2(u)}{v_{\text{gf}}(u) - v_0 \cos \phi} e^{-v_{\text{gf}}^2(u)/v_0^2}, \quad (17)$$

where ϕ is the isotropic angle between the dark matter velocity \vec{v}_{gf} in the galactic frame and the star's velocity \vec{v}_{star} , in the galactic frame. The term v_{gf} satisfies the Galilean transformation:

$$v_{\text{gf}}^2 + v_0^2 - 2v_{\text{gf}}v_0 \cos \phi = u^2. \quad (18)$$

Here, N^* is the normalization factor ensuring $\int du \int d \cos \phi f(u, \phi) = 1$.

As described by Eq. (15), DM particles slower than the maximum initial velocity $v_{\text{max}}(\theta)$ will be captured, eventually falling into the star's core. Thus, the maximum velocity at an infinite distance in the star frame can be derived from a gravitational acceleration:

$$u_{\text{max}}(\theta) = \sqrt{v_{\text{max}}(\theta)^2 - v_{\text{esc}}^2} \quad (19)$$

Then, we derive the average capture rate for dark matter particles, F_{cap} , which is the fraction of DM particles captured by the star:

$$F_{\text{cap}} = \int_0^1 d \cos \theta \int_0^{u_{\text{max}}(\theta)} du \int_{-1}^1 d \cos \phi f(u, \phi). \quad (20)$$

We consider DM in the relatively strong interacting region, so that F_{cap} is very close to 1 for the parameter space of interest, as discussed in [48, 49].

Criterion of gravitational collapse

As outlined in the main text, the dark matter accreted within the star can collapse into a black hole only if it satisfies the following three criteria: Jeans instability, self-gravitating instability, and the Chandrasekhar limit. We follow [48, 49] and discuss these criteria individually below.

In the stable thermal state, before the onset of any instability, dark matter particles reach a virialized distribution with a temperature equal to that of the host star, T_{star} . At this juncture, the dark matter density is sufficiently low to be considered negligible, allowing the star's gravitational potential to be approximated as $V(r) = \frac{2}{3}\pi\rho_{\text{star}}Gm_{\chi}r^2$. According to the Virial Theorem, this potential $\langle V(r) \rangle$ correlates with

the DM kinetic energy $\langle E_k \rangle = \frac{3}{2}T_{\text{star}}$, providing an estimate for the thermal radius r_{th} , within which dark matter can remain gravitationally bound in a virialized thermal state:

$$r_{\text{th}} \approx \sqrt{\frac{9T_{\text{star}}}{4\pi G \rho_{\text{star}} m_\chi}}. \quad (21)$$

Jeans Instability

Jeans instability occurs when the dark matter self-gravitating free-fall time t_{ff} —the time it takes for a dark matter particle to fall from the thermal radius to the star’s center—equals the sound-crossing time t_{sc} , assuming a sound speed $c_s = \sqrt{\frac{T_{\text{star}}}{m_\chi}}$. The free-fall time, given the star’s harmonic gravitational potential, is:

$$t_{\text{ff}} = \sqrt{\frac{3\pi}{16\rho_\chi^{\text{star}} G}}, \quad (22)$$

where ρ_χ^{star} represents the dark matter density within the thermal sphere of the star. The sound-crossing time can be expressed as:

$$t_{\text{sc}} = \frac{r_{\text{th}}}{c_s} = \frac{3}{\sqrt{4\pi G \rho_{\text{star}}}}. \quad (23)$$

Equating t_{ff} and t_{sc} yields:

$$\rho_\chi^{\text{star}} = \frac{\pi^2}{12} \rho_{\text{star}}, \quad (24)$$

leading to a critical mass for the onset of Jeans Instability:

$$M_{\text{crit}}^{\text{JI}}(m_\chi) = \sqrt{\frac{9\pi^3 T_{\text{star}}^3}{64\rho_{\text{star}} G^3 m_\chi^3}}. \quad (25)$$

Self-gravitating Instability

When the mass of accreted dark matter, denoted as M_{acc} , becomes significantly large, the dark matter cannot maintain a virialized state at the star’s temperature. In the absence of sufficient pressure from other interactions, such as the thermal pressure accounted for in the Jeans Instability scenario or the quantum pressure in the Chandrasekhar limit, the dark matter would collapse to form a black hole. The virial theorem for a dark matter particle in a bound state considers both the gravitational potential from the stellar and dark matter contributions as:

$$3T_{\text{star}} = \frac{4}{3}\pi r^2 \rho_{\text{star}} G m_\chi + \frac{GM_{\text{acc}} m_\chi}{r}. \quad (26)$$

A solution for r becomes infeasible when M_{acc} reaches a critical threshold, indicating that no thermal bound state can be formed within radius r without considering additional interactions, signifying gravitational instability. The *r.h.s.* above has a minimum

value at $r = \left(\frac{3M_{\text{acc}}}{8\pi\rho_{\text{star}}}\right)^{1/3}$, which sets the condition for self-gravitating instability:

$$3T_{\text{star}} = \frac{3}{2}Gm_{\chi} \left(\frac{8}{3}\pi\rho_{\text{star}}M_{\text{acc}}^2\right)^{1/3}, \quad (27)$$

leading to the critical mass for instability:

$$M_{\text{crit}}^{\text{SG}}(m_{\chi}) = \sqrt{\frac{3T_{\text{star}}^3}{\pi\rho_{\text{star}}G^3m_{\chi}^3}}. \quad (28)$$

Chandrasekhar Limit

The Chandrasekhar limit defines the mass threshold beyond which quantum degenerate pressure can no longer counteract self-gravity. This criterion must be met to prevent collapse under quantum pressure. For fermionic dark matter, the critical mass is:

$$M_{\text{crit}}^{\text{Ch-F}}(m_{\chi}) \sim \frac{M_{\text{pl}}^3}{m_{\chi}^2}, \quad (29)$$

and for bosonic dark matter:

$$M_{\text{crit}}^{\text{Ch-B}}(m_{\chi}) \sim \frac{M_{\text{pl}}^2}{m_{\chi}}, \quad (30)$$

where $M_{\text{pl}} \sim G^{-1/2}$ represents the Planck mass.

The critical mass conditions for Jeans instability and self-gravitating instability show similar parameter dependencies, albeit with slight differences in coefficients. Therefore, to ascertain the critical mass for dark matter collapse, one must compare the conditions for Jeans instability and the Chandrasekhar limit. Considering a star of mass $3M_{\odot}$ as the least massive star under consideration, the critical mass for Jeans instability, $M_{\text{crit}}^{\text{JI}}(m_{\chi}) \approx 10^{48} \text{ GeV} \left(\frac{m_{\chi}}{10^6 \text{ GeV}}\right)^{-3/2}$ for fermionic dark matter, and $M_{\text{crit}}^{\text{JI}}(m_{\chi}) \approx 1.8 \times 10^{45} \text{ GeV} \left(\frac{m_{\chi}}{10^6 \text{ GeV}}\right)^{-2}$. The scaling relations for temperature and core density in the main sequence stars indicate that an increase in star mass raises the critical mass for Jeans instability but does not alter the Chandrasekhar limit. Additionally, bosonic dark matter exhibits a lower Chandrasekhar limit. Consequently, the Jeans instability criterion predominantly determines the critical mass for dark matter to collapse into a black hole, $M_{\text{crit}} = M_{\text{crit}}^{\text{JI}}$, across most of the parameter space of interest.

Halo mass distribution, dark matter halo, and stellar matter distribution

We utilize the Sheth-Tormen distribution at $z = 0$ for modeling the local galaxy halo mass distribution [60, 62]:

$$M_{\text{h}} \frac{dn}{dM_{\text{h}}} = \Omega_{\text{m},0}\rho_{\text{cr},0} \frac{d\sigma(M_{\text{h}})}{\sigma(M_{\text{h}})dM_{\text{h}}} f(\sigma), \quad (31)$$

where $\Omega_{m,0} \equiv \rho_{m,0}/\rho_{cr,0} \approx 0.3$ represents the current matter energy fraction, and $\rho_{cr,0} \approx 10^{-26} \text{kg/cm}^3$ denotes the current critical energy density. The term $\sigma(M_h)$ indicates the current root-mean-square (rms) density fluctuation, which is modeled using numerical simulations from the Bolshoi simulations, incorporating observational parameters from WMAP5 and WMAP7 data [80–82]:

$$\sigma(M_h) = \frac{16.9y^{0.41}}{1 + 1.102y^{0.20} + 6.22y^{0.333}}, \quad (32)$$

$$y \equiv \left[\frac{M_h}{10^{12} h^{-1} M_\odot} \right]^{-1}.$$

The function $f(\sigma)$ represents the modified analytic fit of first-crossing distribution function, which assumed to be an adaptation of the original Press-Schechter function, refined by [81]:

$$f(\sigma) = A_f \sqrt{\frac{2b_f}{\pi}} \left[1 + \left(\frac{b_f}{\sigma^2} \right)^{-0.3} \right] \frac{1}{\sigma} \exp\left(-\frac{b_f}{2\sigma^2}\right), \quad (33)$$

$$A_f = 0.322, \quad b_f = 2.01.$$

The structure of the dark matter halo is characterized by a Navarro-Frenk-White (NFW) profile [58]:

$$\rho_\chi(r_g) = \frac{\rho_0}{r_g/R_s (1 + r_g/R_s)^2}, \quad (34)$$

where r_g is the radial distance from the center of the halo, and R_s is the scale radius linked to the virial radius R_{vir} through the concentration parameter $C(M_h) = R_{\text{vir}}/R_s$. The concentration parameter, based on the Bolshoi and MultiDark simulation data for $z \approx 0$, is described as [82]:

$$C(M_h) = A_C \left[\left(\frac{\sigma(M_h)}{b_C} \right)^{c_C} + 1 \right] \exp\left(\frac{d_C}{\sigma(M_h)^2}\right), \quad (35)$$

$$A_C = 2.881, \quad b_C = 1.257, \quad c_C = 1.022, \quad d_C = 0.06.$$

The virial radius is defined as the radius within which the average density of the halo is Δ times the critical energy density, with Δ typically set to 200 [83]:

$$R_{\text{vir}} = \sqrt[3]{\frac{3M_h}{4\pi\Delta\rho_{cr,0}}}. \quad (36)$$

Consequently, R_s is expressed as a function of the halo mass M_h , allowing for the determination of ρ_0 through the normalization of the halo mass:

$$M_h = \int_0^{R_{\text{vir}}} \rho_\chi(r_g) 4\pi r_g^2 dr_g. \quad (37)$$

However, it's noted that the Milky Way's halo does not perfectly align with this model due to its complex structure and history [84].

With the halo mass distribution established, we estimate the total stellar mass M_s in local galaxies (at $z \approx 0$) with a halo mass of $M_h \equiv xM_0$, following the methodology in [59, 60]:

$$\log_{10} \left(\frac{M_s}{M_0} \right) = \epsilon_0 - \log_{10} (10^{-\alpha_0 x} + 10^{-\beta_0 x}) + \gamma_0 \exp^{-\frac{1}{2} \left(\frac{x}{\delta_0} \right)^2}, \quad (38)$$

where $M_0 = 10^{12.06} M_\odot$, $\epsilon_0 = -1.459$, $\alpha_0 = 1.972$, $\beta_0 = 0.488$, $\gamma_0 = 10^{-0.958}$, $\delta_0 = 0.391$.

In this paper, we adopt two typical structures for the stellar matter in galaxies: elliptical and disk.

We employ the Hernquist Model [85] to describe the isotropic distribution of elliptical galaxies:

$$\rho_s^e(r_g) = \frac{C^e}{2\pi} \frac{R^e}{r_g(r_g + R^e)^3}, \quad (39)$$

where r_g represents the radial distance from the center of the halo, and R^e , related to the half-mass radius, is defined as $R^e = R_{1/2}/(1 + \sqrt{2})$.

For disk galaxies, the stellar matter distribution is modeled using an exponential disk profile [60, 86]:

$$\rho_s^d(R_g, h_g) = C^d \exp\left(-\frac{R_g}{R^d}\right) \exp\left(-\frac{|h_g|}{h^d}\right), \quad (40)$$

where (R_g, h_g) denote the cylindrical coordinates in the galaxy, with R^d and h^d being the characteristic scale lengths related to the galaxy's half-mass radius: $R^d \approx R_{1/2}/1.68$ and $h^d \approx R_{1/2}/10$.

In both cases, the half-mass radius of the halo is proportionate to the virial radius, expressed as $R_{1/2} \approx 0.015 R_{\text{vir}}$ [87]. The normalization of the total stellar mass for both profiles is used to determine the normalization constants C^e and C^d :

$$M_s = \int \rho_s^{e(d)}(\vec{r}) d^3 \vec{r}, \quad (41)$$

where the integration is performed over the entire volume of the galaxy.

Modification to the relative binary formation rate

Here, we analyze the effects of black hole (BH) mass on the relative formation rates of BH-Neutron Star (NS) binaries, highlighting two primary factors.

Firstly, BHs of varying mass ranges exhibit distinct number densities. This variance stems from the progenitor stars' adherence to an Initial Mass Function (IMF) [61]:

$$\frac{dn_{\text{star}}}{dM_{\text{star}}} \propto M_{\text{star}}^{-2.3}, \quad 0.5M_\odot \leq M_{\text{star}} < 100M_\odot, \quad (42)$$

assuming $M_{\text{LMBH}} = M_{\text{star}}$ for lower mass black holes, which accrete the majority of their progenitor star's mass, and $M_{\text{ABH}} = \frac{1}{4}M_{\text{star}}$ to account for mass loss during the evolution of more massive stars.

Secondly, for a BH-NS binary with a given initial orbital separation, the merger occurs more rapidly with increasing BH mass due to enhanced gravitational wave (GW) emission. This impacts the observed merger rates for GW detectors over observation periods of the order of 1 year. The orbital period's maximum value, allowing for a merger within $\Delta t^{\text{ob}} = 1$ year, is given by [74]

$$P_{\text{max}}^{\text{ob}}(M_{\text{BH}}) \approx \left(\frac{256\pi^{8/3} \Delta t^{\text{ob}} G^{5/3} M_{\text{BH}} M_{\text{NS}}}{5(M_{\text{BH}} + M_{\text{NS}})^{1/3}} \right)^{8/3}, \quad (43)$$

with the period distribution for close binary systems modeled as a Gaussian centered at $\log_{10}(P/\text{day}) = 4.8$ with a dispersion of 2.3 [75].

Integrating over the IMF and binary period distribution, we determine the modification to the merge rate ratio A :

$$A = \frac{\int_{3M_{\odot}}^{5M_{\odot}} \frac{dn_{\text{star}}}{dM_{\text{star}}} dM_{\text{star}} \int_{\log P_{\text{min}}^{\text{ob}}(M_{\text{star}})}^{\log P_{\text{max}}^{\text{ob}}(M_{\text{star}})} \frac{dn}{d\log P} d\log P}{\int_{20M_{\odot}}^{80M_{\odot}} \frac{dn_{\text{star}}}{dM_{\text{star}}} dM_{\text{star}} \int_{\log P_{\text{min}}^{\text{ob}}(M_{\text{star}})}^{\log P_{\text{max}}^{\text{ob}}(M_{\text{star}}/4)} \frac{dn}{d\log P} d\log P}, \quad (44)$$

yielding $A = 5.79$, under the assumption that $M_{\text{NS}} = 1.5M_{\odot}$ in all cases. This ratio highlights the significant impact of BH mass on BH-NS binary formation rates.

Acknowledgements. We thank Anil Seth, Dan Wik, Gail Zasowski and Zheng Zheng for useful discussions. This work is supported by the National Key Research and Development Program of China under Grant No. 2020YFC2201501. S.G. is supported by the National Natural Science Foundation of China under Grant No. 12247147. J.S. is supported by Peking University under startup Grant No. 7101302974 and the National Natural Science Foundation of China under Grants No. 12025507, No.12150015; and is supported by the Key Research Program of Frontier Science of the Chinese Academy of Sciences (CAS) under Grants No. ZDBS-LY-7003. Y.Z. is supported by the U.S. Department of Energy under Award No. DESC0009959.

Author Contributions: J.S. and Y.Z. initiated this study, S.G. and Y.L. performed the calculations. S.G. and Y.L. wrote the initial draft, with contributions from J.S. and Y.Z.. All authors have reviewed, discussed and commented on the calculations and manuscript.

Competing interests: The authors declare that they have no competing interests.

Data and materials availability: All data needed to evaluate the conclusions in the paper are present in the paper.